Biomedical Research 2016; 27 (3): 737-742

ISSN 0970-938X
www.biomedres.info

The effects of hesperidin on idiopathic pulmonary fibrosis evaluated by histopathologial-biochemical and micro-computed tomography examinations in a bleomycin-rat model.

Cemile Ayşe Görmeli[1*], Kaya Saraç[1], Osman Çiftçi[2], Necati Timurkaan[3], Sıddık Malkoç[4]

[1]Department of Radiology, Inonu University School of Medicine, Malatya, Turkey

[2]Department of Pharmacology, Inonu University School of Medicine, Malatya, Turkey

[3]Department of Pathology, Fırat University Veterinary Medical School, Elazığ, Turkey

[4]Department of Orthodontics, Inonu University Faculty of Dentistry, Malatya, Turkey

Abstract

Idiopathic Pulmonary Fibrosis (IPF) is a chronic, progressive parenchymal lung disease. The pathology is characterized by recurrent injury to microscopic alveolar epithelial cells. These injuries activate inflammatory cells, resulting in the proliferation of fibroblasts and alveolar tissue damage. Interstitial inflammation, advanced oxidative stress, and abnormal antioxidant activity were demonstrated to be the main causes of IPF. Hesperidin (HP) is a bioflavonoid with anti-inflammatory, antioxidant, anticarcinogenic, and analgesic actions. HP may be able to prevent pulmonary fibrosis, and may ultimately lead to healthy lung function. We hypothesized that HP could prevent Bleomycin (BLC)-induced pulmonary fibrosis due to its biochemical, antioxidant, and anti-inflammatory properties and may ultimately lead to healthy lung function. Based on these findings, we hypothesized that HP could prevent BLC-induced pulmonary fibrosis due to its biochemical, antioxidant, and anti-inflammatory properties. The animals were divided into 4 groups with 14 rats per group. The experimental treatments were as follows: Control, BLC, HP, and BLC+HP. Six of the 14 lungs in each group were sent for micro-CT analysis. The remaining 8 lung specimens were harvested for histopathological and biochemical analyses. BLC-treated rats showed marked histopathological changes in the lungs. In these rats, thickening of interalveolar septa due to macrophage and lymphocyte infiltration, as well as fibroblast proliferation, were observed. Histopathological changes were less severe in the BLC+HP group compared with the BLC group. HP treatment led to a decrease in lipid peroxidation and an increase in antioxidant status compared with the BLC group. Also micro-CT showed a significant positive correlation with histopathological and biochemical results. To the best of our knowledge, this is the first study to evaluate the beneficial effects of HP against pulmonary fibrosis using histopathological, biochemical, and micro-CT analyses and HP successfully minimized the severity of BLC-induced lung injury, which was used as a model for IPF.

Keywords: Idiopathic pulmonary fibrosis, Micro-computed tomography, Hesperidin.

Accepted on February 25, 2016

Introduction

Idiopathic Pulmonary Fibrosis (IPF) is a chronic, diffuse, progressive parenchymal lung disease and is the most common form of interstitial pneumonia [1]. The incidence of IPF is 6.8-8.8 cases per 100,000 [2]. This progressive lung disease has a poor prognosis with a median survival of only 2-3 years. The pathology is characterized by recurrent injury to microscopic alveolar epithelial cells. These injuries activate inflammatory cells, which release harmful amounts of Reactive Oxygen Species (ROS), resulting in the proliferation of fibroblasts and alveolar tissue damage [3]. Myeloperoxidase is an enzyme that is released from activated neutrophils and interacts with Hydrogen Peroxide (H_2O_2), which then forms highly toxic hydroxyl radicals [4]. Repetitive injury, failed repair, fibrosis, and deposition of extreme Extracellular Matrix (ECM) result in pathologic tissue scarring that negatively affects parenchymal architecture. In addition, interstitial inflammation, advanced oxidative stress, and abnormal antioxidant activity were demonstrated to be the main causes of IPF [5,6]. Therefore, as an adjuvant therapy, supplementing patients with anti-inflammatory and antioxidant agents may help prevent and treat IPF.

Animal models of lung fibrosis have been useful for understanding the fibrotic process. Bleomycin (BLC)-induced pulmonary fibrosis is the most widely used animal model of human IPF. Intratracheal application of BLC causes the proliferation of fibroblasts, an inflammatory response in alveolar epithelial cells, and the deposition of collagen [7,8]. In this study, antioxidant agents were tested in a BLC-induced lung fibrosis animal model, and were found to be beneficial in preventing fibrosis [9-11].

Flavonoids are a class of plant pigments, and Hesperidin (HP) is a bioflavonoid with anti-inflammatory, antioxidant, anti-carcinogenic, and analgesic actions [12,13]. In addition, HP was found to be protective against the toxic effects of cisplatinum in rat eyes, and was reported to activate antioxidant function with its strong free oxygen radical scavenging activity [14] thus, HP may be able to prevent pulmonary fibrosis caused by interstitial inflammation and advanced oxidative stress due to its anti-inflammatory and anti-oxidative properties, and may ultimately lead to healthy lung function.

Based on these findings, we hypothesized that HP could prevent BLC-induced pulmonary fibrosis due to its biochemical, antioxidant, and anti-inflammatory properties. Therefore, we investigated oxidative status, histopathological changes, and micro-Computed Tomography (micro-CT) in the lungs of rats.

Materials and Methods

Chemicals

BLM was obtained from Onko Medical Company (BLEOCIN-S®, 15 mg, Istanbul, Turkey) and HP was obtained from Molecula Limited (Gillingham, UK). All other chemicals were purchased from Sigma Chemical Co. (St Louis, MO, USA) and were either analytical grade or the highest grade available.

Study design

This experimental study was approved by the Animal Ethics committee (reference number, 2014/A-81). Experiments were performed based on the Animal Welfare Act and the Guide for the Care and Use of Laboratory animals (National Institutes of Health [NIH] publication No. 5377-3, 1996), Local Animal Ethics Committee. In total, 42 healthy adult male Sprague-Dawley rats (3-4 months of age and 250-300 g in weight) were obtained from the Experimental Animal Institute, Malatya, Turkey. The animals were placed in sterilized polypropylene rat cages, and housed in a room maintained at 21 ± 2°C and 60 ± 5 % humidity, with a 12-h light-dark cycle.

The animals were randomly divided into 4 groups with 14 rats per group. The experimental treatments were as follows: Control, BLC, HP, and BLC + HP. Rats in the control group received intratracheal injection (2.5 mg/kg body weight) in 0.25 mL Phosphate Buffered Saline (PBS) using corn oil as a vehicle. In the BLC group, a single intratracheal injection of BLC hydrochloride (2.5 mg/kg body weight) in 0.25 mL PBS was administered while the rats were anesthetized to achieve lung fibrosis. In the HP group, 50 mg/kg/day HP was given by gavage for 14 consecutive days. In the BLC+HP group, 50 mg/kg oral HP was given 1 day before the intratracheal BLC injection and continued for 14 days. This procedures were applied as the similar studies that presented before [11,14]. Fourteen days after the BLC injection, all rats were sacrificed by an overdose of anesthesia. Six of the 14 lungs in each group were sent for micro-CT analysis. The remaining 8 lung specimens were harvested for histopathological and biochemical analyses. The right section of each lung was placed in liquid nitrogen and stored at -70°C until tested for Thiobarbituric Acid Reactive Substances (TBARS), Catalase (CAT), Superoxide Dismutase (SOD), Glutathione Peroxidase (GPx), and reduced Glutathione (GSH). The left section of each lung was placed in formaldehyde prior to histopathological evaluation under light microscopy. Previous dose-response studies on anti-inflammatory and anti-oxidative effects in rats and lung fibrosis were used to choose the HP and BLC doses [15-17].

Micro-CT scanning and image analysis

After sacrifice, 5 mL of air was introduced into the trachea using a syringe. The trachea was then bound to prevent air leakage. The lungs were extracted and scanned using a desktop micro-CT system (SkyScan 1072; SkyScan, Contich, Belgium) to evaluate and quantify the total lung injury area.

Each specimen was mounted on the computer-controlled turntable such that the x-ray beam was perpendicular to the horizontal axes of the rat lung. Digital section images were acquired under the following conditions: 100 mA beam current, 100 kV accelerating voltage, 0.5 mm aluminum filter, 27.37 µm pixel size at 1,000 × 1,000 resolution, and 180° rotation at the 0.3° step. About 650-700 cross-sectional images were taken from each sample using an 11 Mp camera. The full scan time duration was 55-60 min. All three-dimensional (3D) images were evaluated on a 17-inch TFT computer screen by the same operator.

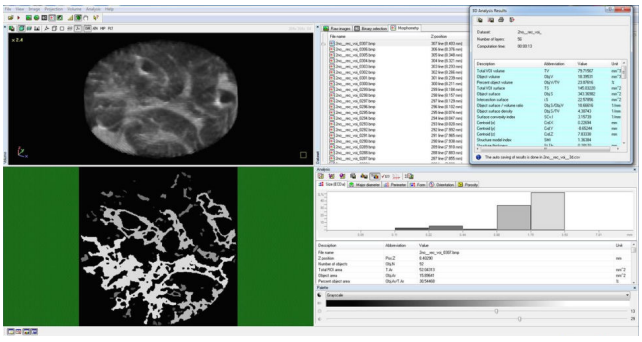

Figure 1. *Evaluation of micro-CT images.*

The micro-CT images were evaluated using the CTAn 1.13.5.1 program (SkyScan, Kontich, Belgium). Ground glass densities and peripheral patchy consolidation indicated lung injury. The right and left lower zones of the lungs were separated and cylinder shapes (each 1.5 mm × 8 mm) were chosen as the

Regions of Interest (ROIs). The CTAn 1.13.5.1 program (SkyScan, Kontich, Belgium) was used to analyze the multiplanar images in the axial, coronal, and sagittal planes for each reconstructive lung image, and to calculate the lung injury volume fraction (injury volume/total volume) (Figure 1).

Biochemical assays

Tissue was homogenized in a Teflon glass homogenizer in 150 mM KCl (pH 7.4) to obtain a 1: 10 (w/v) dilution of the whole homogenate. The homogenates were centrifuged at 18,000 g (4°C) for 30 min to determine TBARS content, reduced Glutathione (GSH) concentration, and CAT activity, and at 25,000 g for 50 min to determine glutathione peroxidase (GSH-Px) activity. The levels of TBARS, an indicator of lipid peroxidation, were determined in 1 g homogenized lung tissue by the thiobarbituric acid reaction using previously described methods [18]. The product was evaluated spectrophotometrically at 532 nm and the results were expressed as nmol/g tissue. The reduced GSH content of the lung homogenate was measured at 412 nm using the methods of Sedlak and Lindsay [19]. GSH levels were expressed as nmol/mL. CuZn-SOD activity was measured by the inhibition of Nitroblue Tetrazolium (NBT) reduction due to O_2^- generated by the xanthine/xanthine oxidase system [20]. One unit of SOD activity was defined as the amount of protein resulting in 50% inhibition of the NBT reduction rate. The product was evaluated spectrophotometrically at 560 nm. Results are expressed as IU/mg protein.

CAT activity was determined according to the method of Aebi et al. [21]. The enzymatic decomposition of H_2O_2 was followed directly by a decrease in absorbance at 240 nm. The difference in absorbance per unit time was used as a measure of CAT activity. The enzyme activities are shown in kU/mg protein. GSH-Px activity was measured using the methods of Paglia and Valentina [22]. In the presence of glutathione reductase and NADPH, the oxidized Glutathione (GSSG) is immediately converted to the reduced form with a concomitant oxidation of NADPH to NADP. The decrease in absorbance at 340 nm was measured. GSH-Px activity was expressed as IU/mg protein. Tissue protein content was determined according to the method developed by Lowry et al. [23], using Bovine Serum Albumin (BSA) as the standard.

Histopathological examination

After sacrifice, the lungs were removed and fixed in 10% neutral buffered formalin. The lung tissues (3 specimens/animal) were processed for routine paraffin embedding, and sectioned at a 5 µm thickness. The cross sections were stained with hematoxylin & eosin for histological examination. The scoring system described by Ashcroft et al. [24], was used to estimate the severity of pulmonary fibrosis on a numerical scale (Table 1). Using a 10X objective, an average of 10 fields per slide were assessed for pulmonary fibrosis severity. Each field was assigned a score between 0 (normal lung) and 8 (total fibrosis). The mean of the scores for all fields was taken as the fibrotic score of the section.

Table 1. *Criteria for grading lung fibrosis described by Ashcroft et al.*

Score	Histological features
0	Normal lung
1	Minimal fibrous thickening of alveolar or bronchiolar walls
2	Moderate thickening of walls without obvious damage to lung architecture
3	
4	Increased fibrosis with definite damage to lung structure and formation of fibrous bands or smallfibrous masses
5	
6	Severe distortion of structure and large fibrous areas
7	
8	Total fibrous obliteration of the field

Table 2. *Lung fibrosis score in the experimental groups.*

Groups	Case numbers	Scores of the lung fibrosis	P-value
Control	5	0^x	0.001
H	5	0^x	
B	5	3.24 ± 0.35^y	
B+H	5	1.71 ± 1.20^y	

Means bearing different superscripts within same column were significantly different (P<0.05).

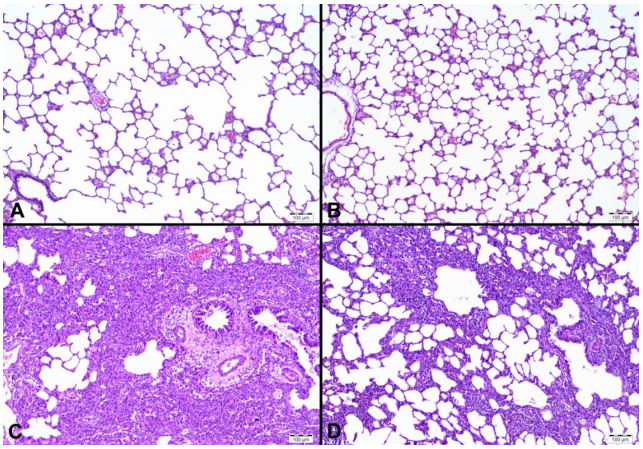

Figure 2. *A and B. Photomicrographs showing the normal histological appearance of the lungs in the control (A) and the HP-only group (B) rats. Hematoxylin and eosin.C. Photomicrograph of the lung of a rat in the BLC-only group showing the thickening of the interalveolar septa by mononuclear cell infiltration and fibroblast proliferation. Hematoxylin and eosin.D. Photomicrograph of the lung of a rat in the BLC+HP group. Note that the histopathological changes were less severe compared with the BLC-only group (C). Hematoxylin and eosin. Abbreviations : HP; hesperidin, BLC; Bleomycin.*

Statistics

Data analysis was performed using IBM SPSS Statistics 22.0 (IBM, Armonk, NY, USA). Data are presented as the median (min-max). The Kruskal-Wallis test was used to statistically evaluate the data among the groups. The Conover multiple comparison test was used to differentiate one group from the other. A P-value<0.05 was considered statistically significant.

Results

Histopathological findings

The lung tissue sections of the control and HP-treated groups showed normal histological structure (Figures 2A and 2B). BLC-treated rats showed marked histopathological changes in the lungs. In these rats, thickening of interalveolar septa due to macrophage and lymphocyte infiltration, as well as fibroblast proliferation, were observed (Figure 2C). Neutrophils were observed in both the alveoli and intersititium. The alveolar architecture was damaged by desquamation of type I pneumocytes, proliferation of type II pneumocytes, and accumulation of foamy macrophages. Emphysematous changes, including fragmentation of alveolar septa and expansion of alveolar spaces, were also seen. Histopathological changes were less severe in the BLC+HP group compared with the BLC group (Figure 2D).The BLC group had the highest Ashcroft fibrosis score (3.24 ± 0.35). Although there was a marked reduction in fibrosis between the BLC and BLC+HP groups (Ashcroft score: 1.71 ± 1.20) the difference was not statistically significant (Table 2).

Biochemical results

The SOD, GPx, GSH, and TBARS levels are shown in table 3. BLC treatment resulted in a significant increase in the TBARS levels and a significant decrease in the SOD, GPx, and GSH levels compared with the other groups. The TBARS levels and SOD activity were significantly different in the HP-treated groups compared with the control group. There were no significant changes in oxidant/antioxidant parameters between the control and HP groups. Additionally, BLC+HP combined led to a significant decrease in the TBARS levels, and a significant increase in SOD, GPx, and GSH levels. HP treatment led to a decrease in lipid peroxidation and an increase in antioxidant status compared with the BLC group.

Micro-CT findings

The severity of lung injury was 1.52% in the control group and 1.75% in the HP group due to traumatic damage caused while harvesting (Figures 3A and 3B). There were no significant differences in the lesion size between these groups. In the BLC group, the lung injury volume fraction was 14.4%. The BLC +HP group showed reduced fibrosis severity with a score of 4.38% (Figures 3C and 3D), which was significantly different from the BLC group (Figure 4).

Table 3. *The levels of SOD, GSH and TBARS in rat lung tissue (Mean ± SD).*

	TBARS (nmol/g tissue)	Reduced GSH nmol/ml	SOD (U/mg protein)	GPx (U/mg protein)
Control	8.81 ± 0.68^{a}	51.5 ± 8.95^{a}	30.1 ± 4.74^{a}	221.5 ± 14.2^{a}
Hesperidin	5.36 ± 0.74^{b}	52.5 ± 4.01^{a}	29.0 ± 3.00^{b}	219.5 ± 22.1^{a}
Bleomycin	13.2 ± 0.84^{c}	35.7 ± 5.24^{b}	17.2 ± 1.21^{c}	141.2 ± 13.0^{b}
Bleomycin+hesperidin	10.1 ± 1.24^{d}	41.6 ± 3.83^{c}	22.4 ± 2.31^{d}	178.5 ± 21.1^{c}

Means with different superscripts within the same column were significantly different (P<0.01). SOD: Superoxide Dismutase, GSH: reduced Glutathione, TBARS: Thiobarbituric Acid Reactive Substances, SD: Standard Deviation

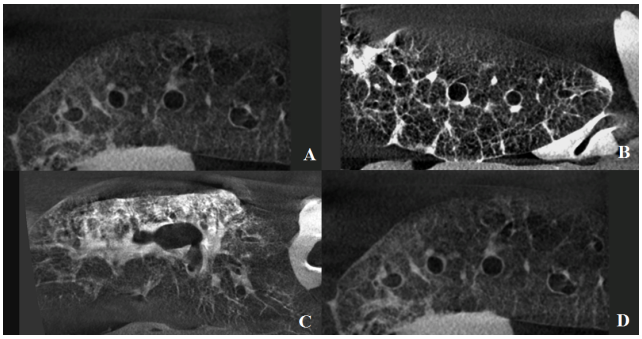

Figure 3. *Severity of lung injury in control (A), HP (B), BLC (C) and BLC+HP (D) groups.*

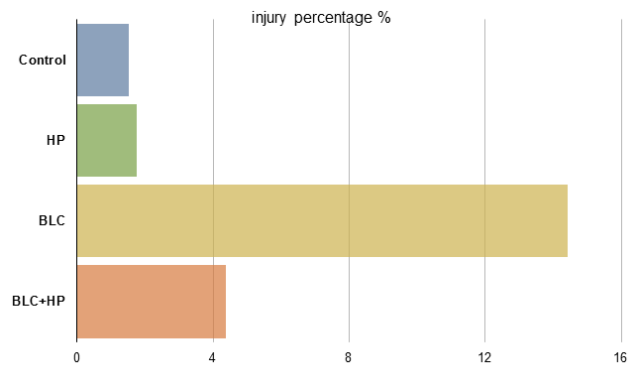

Figure 4. *Comparison of lung injury evaluated via micro-CT between groups. HP: Hesperidin, BLC: Bleomycin.*

Discussion

To the best of our knowledge, this is the first study to evaluate the beneficial effects of HP against pulmonary fibrosis using histopathological, biochemical, and micro-CT analyses. This study demonstrated that HP treatment has promising preventive effects on BLC-induced lung fibrosis. BLC causes the proliferation of fibroblasts, an inflammatory response in alveolar epithelial cells, and the deposition of collagen [7,8]. BLC-induced pulmonary fibrosis is a widely used and well-established model of IPF [25]. There are several dosing methods; however, intratracheal BLC administration is the most popular mode of administration. Lung injury occurs after the generation of oxidant species through iron-dependent mechanisms. Type I alveolar epithelial cell death occurs and is followed by inflammation during the first 7 days, which mimics acute lung injury. The inflammatory response period continues for 14 days. The inflammation then resolves, and fibrosis occurs within 3 days. After 3-4 weeks of BLC administration, the fibrotic stage begins with intense deposition of ECM [26]. Organisms maintain a balance between free radicals and antioxidants to prevent oxidative stress [27]. Imbalances in this mechanism result in exposure to free radicals with an inadequate defense mechanism, and may lead to pulmonary fibrosis [28]. TBARS, which forms due to fatty acid peroxidation with reactive oxygen radicals, reflects lipid peroxidation in the cell. Lipid oxidation can result in irreversible cell membrane damage [29]. The increased TBARS levels in BLC-treated rats demonstrate that lipid peroxidation occurs in this study. Interestingly TBARS levels were significantly decreased in the HP+BLC group compared with the BLC group, likely due to the radical scavenging and antioxidant properties of HP. SOD, GPx, and CAT are the main defense enzymes and GSH is the main non-enzymatic defense against lipid peroxidation [10,30]. SOD forms H_2O_2 from superoxide radical anions. The H_2O_2 is then reduced to water by CAT and GPx [31]. Increased antioxidant enzyme levels were found in the HP-treated groups in this study and in several previous studies [14,32,33]. In this study, BLC-treated rats had significantly decreased SOD, GPx, and CAT activities compared with the control group. The levels of these antioxidant enzymes were significantly increased in the groups treated with HP. These findings suggest that HP promotes antioxidant activity. GSH is a major thiol tripeptide that plays an important role in the antioxidant mechanisms in the cell [34]. GSH is a cofactor for enzymes that prevent oxidative stress, transport amino acids from the basal membrane, scavenge free radicals, and regenerate vitamins C and E to their active forms [34]. Previous studies showed that decreased GSH levels by BLC is a risk factor for lung fibrosis, and that antioxidants can alter the GSH levels [7,11]. In this study, HP treatment successfully reversed GSH depletion in BLC-treated animals. In addition, similar results have been found when using HP to treat cisplatin-induced ocular toxicity and in a cerebral ischemia/reperfusion model [13,14]. This study demonstrated that BLC treatment resulted in significant histopathological alterations in the lung, including thickening of interalveolar septa through macrophage and lymphocyte infiltration, and fibroblast proliferation. HP treatment markedly attenuated these effects in BLC-treated animals. These findings are in agreement with previous studies that used antioxidant agents to treat BLC-induced lung injury [11,34]. Furthermore, this study showed that lung injury could be evaluated using micro-CT with high accuracy compared with histopathological and biochemical techniques. Although there was no significant difference between the micro-CT image analysis of the HP and control groups, there was a difference between the BLC and BLC+HP groups. While the BLC group showed significant lung injury, a considerable decrease in injury area was observed in the BLC+HP group. These results may eliminate the need for redundant biopsies in clinical trials for IPF treatment. A parallel study [35,36] showed that micro-CT was a useful method in determining lung injury, and was as accurate as histopathological techniques. However, more study is needed.

Conclusion

In conclusion, HP successfully minimized the severity of BLC-induced lung injury, which was used as a model for IPF. The positive effects of HP were evaluated through histopathological, biochemical, and micro-CT examinations. The minimizing effect of HP in pulmonary fibrosis would be a promising report for the treatment of IPF for further investigations.

Acknowledgement

We acknowledge,the support of IUBAP (Scientific Research Fund of Inonu University) under Grant 2015/56.

References

1. Raghu G, Collard HR, Egan JJ. An official ATS/ERS/JRS/ALAT statement: idiopathic pulmonary fibrosis: evidence-based guidelines for diagnosis and management. Am J Respir Crit Care Med 2011; 183: 788-824.
2. Nalysnyk L, Cid-Ruzafa J, Rotella P, Esser D. Incidence and prevalence of idiopathic pulmonary fibrosis: review of the literature. Eur Respir Rev 2012; 21: 355-361.
3. Fernandez IE, Eickelberg O. New cellular and molecular mechanisms of lung injury and fibrosis in idiopathic pulmonary fibrosis. Lancet 2012; 380: 680-688.
4. Dedon PC, Goldberg IH. Free-radical mechanisms involved in the formation of sequence-dependent bistranded DNA lesions by the antitumor antibiotics bleomycin, neocarzinostatin, and calicheamicin. Chem Res Toxicol 1992; 5: 311-332.
5. Bringardner BD, Baran CP, Eubank TD, Marsh CB. The role of inflammation in the pathogenesis of idiopathic pulmonary fibrosis. Antioxid Redox Signal 2008; 10: 287-301.
6. Kliment CR, Oury TD. Oxidative stress, extracellular matrix targets, and idiopathic pulmonary fibrosis. Free Radic Biol Med 2010; 49: 707-717.

7. Kilic T, Parlakpinar H, Polat A, Taslidere E, Vardi N. Protective and therapeutic effect of molsidomine on bleomycin-induced lung fibrosis in rats. Inflammation 2014; 37: 1167-1178.
8. Sogut S, Ozyurt H, Armutcu F, Kart L, Iraz M. Erdosteine prevents bleomycin-induced pulmonary fibrosis in rats. Eur J Pharmacol 2004; 494: 213-220.
9. Ermis H, Parlakpinar H, Gulbas G, Vardi N, Polat A. Protective effect of dexpanthenol on bleomycin-induced pulmonary fibrosis in rats. Naunyn Schmiedebergs Arch Pharmacol 2013; 386: 1103-1110.
10. Iraz M, Erdogan H, Kotuk M, YaÄŸmurca M, Kilic T. Ginkgo biloba inhibits bleomycin-induced lung fibrosis in rats. Pharmacol Res 2006; 53: 310-316.
11. Kilic T, Ciftci O, Cetin A, Kahraman H. Preventive effect of chrysin on bleomycin-induced lung fibrosis in rats. Inflammation 2014; 37: 2116-2124.
12. Menze ET, Tadros MG, Abdel-Tawab AM, Khalifa AE. Potential neuroprotective effects of hesperidin on 3-nitropropionic acidinduced neurotoxicity in rats. Neurotoxicology 2012; 33: 1265-1275.
13. Shagirtha K, Pari L. Hesperetin, a citrus flavonone, protects potentially cadmium induced oxidative testicular dysfunction in rats. Ecotoxicol Environ Saf 2011; 74: 2105-2111.
14. Polat N, Ciftci O, Cetin A, Yalmaz T. Toxic effects of systemic cisplatin on rat eyes and the protective effect of hesperidin against this toxicity. Cutan Ocul Toxicol 2016; 35: 1-7.
15. Boyaci H, Maral H, Turan G, Basyiqit I, Dillioqluqil MO. Effects of erdosteine on bleomycin-induced lung fibrosis in rats. Mol Cell Biochem 2006; 281: 129-137.
16. Balakrishnan A, Menon VP. Antioxidant properties of hesperidin in nicotine-induced lung toxicity. Fundam Clin Pharmacol 2007; 21: 535-546.
17. Oztanir MN, Ciftci O, Cetin A, Aladag MA. Hesperidin attenuates oxidative and neuronal damage caused by global cerebral ischemia/reperfusion in a C57BL/J6 mouse model. Neurol Sci 2014; 35: 1393-1399.
18. Yagi K. Simple assay for the level of total lipid peroxides in serum or plasma. Methods Mol Biol 1998; 108: 101-106.
19. Sedlak J, Lindsay RH. Estimation of total, protein-bound, and nonprotein sulfhydryl groups in tissue with Ellman's reagent. Anal Biochem 1968; 25: 192-205.
20. Sun Y, Oberley LW, Li Y. A simple method for clinical assay of superoxide dismutase. Clin Chem 1988; 34: 497-500.
21. Aebi H. Catalase. In Bergmeyer HU (Eds). Methods of Enzymatic Analysis. Academic Press New York 1974; 673-677.
22. Paglia DE, Valentine WN. Studies on the quantitative and qualitative characterization of erythrocyte glutathione peroxidase. J Lab Clin Med 1967; 70: 158-169.
23. Lowry OH, Rosebrough NJ, Farr AL, Randall RJ. Protein measurement with the Folin phenol reagent. J Biol Chem 1951; 193: 265-275.
24. Ashcroft T, Simpson JM, Timbrell V. Simple method of estimating severity of pulmonary fibrosis on a numerical scale. J Clin Pathol 1988; 41: 467-470.
25. Song JS, Kang CM, Kang HH, Yoon HK, Kim YK. Inhibitory effect of CXC chemokine receptor 4 antagonist AMD3100 on bleomycin induced murine pulmonary fibrosis. Exp Mol Med 2010; 42: 465-472.
26. Williamson JD, Sadofsky LR, Hart SP. The pathogenesis of bleomycin-induced lung injury in animals and its applicability to human idiopathic pulmonary fibrosis. Exp Lung Res 2015; 41: 57-73.
27. Valko M, Leibfritz D, Moncol J, Cronin MT, Mazur M, Telser J. Free radicals and antioxidants in normal physiological functions and human disease. International J Biochem Cell Biol 2007; 39: 44-84.
28. MacNee W, Rahman I. Oxidants/antioxidants in idiopathic pulmonary fibrosis. Thorax 50 Suppl 1: S53-58.
29. Pisoschi AM, Pop A. The role of antioxidants in the chemistry of oxidative stress: A review. Eur J Med Chem 2015; 97: 55-74.
30. Schiller HJ, Reilly PM, Bulkley GB. Tissue perfusion in critical illnesses. Antioxidant therapy. Crit Care Med 1993; 21: S92-102.
31. Ghezzi P, Bonetto V, Fratelli M, Thiol-disulfide balance: from the concept of oxidative stress to that of redox regulation, Antioxid. Redox Signal 2005; 7; 964e972.
32. Siddiqi A, Nafees S, Rashid S, Sultana S, Saidullah B. Hesperidin ameliorates trichloroethylene-induced nephrotoxicity by abrogation of oxidative stress and apoptosis in wistar rats. Mol Cell Biochem 2015; 406: 9-20.
33. Ciftci O, Ozcan C, Kamisli O, Cetin A, Basak N, Aytac B. Hesperidin, a Citrus Flavonoid, Has the Ameliorative Effects Against Experimental Autoimmune Encephalomyelitis (EAE) in a C57BL/J6 Mouse Model. Neurochem Res 2015; 40: 1111-1120.
34. Alanazi AM, Mostafa GA, Al-Badr AA. Glutathione. Profiles Drug Subst Excip Relat Methodol 2015; 40: 43-158.
35. Masella R, Di Benedetto R, Varì R, Filesi C, Giovannini C. Novel mechanisms of natural antioxidant compounds in biological systems: involvement of glutathione and glutathione-related enzymes. J Nutr Biochem 2005; 16: 577-586.
36. Choi JS, Jou SS, Oh MH, Kim YH, Park MJ. The dose of cyclophosphamide for treating paraquat-induced rat lung injury. Korean J Intern Med 2013; 28: 420-427.

***Correspondence to:**

Cemile Ayşe Görmeli

Department of Radiology

Inonu University School of Medicine

Turkey